Engineering 39 (2024) 194–203

Contents lists available at ScienceDirect

Engineering

journal homepage: www.elsevier.com/locate/eng

Research
Civil Engineering—Article

A New Dynamic and Vertical Photovoltaic Integrated Building Envelope for High-Rise Glaze-Facade Buildings

Wuwei Zou [b], Yan Wang [b], Enze Tian [c,d], Jiaze Wei [b], Jinqing Peng [e,*], Jinhan Mo [a,b,f,g,h,*]

[a] College of Civil and Transportation Engineering, Shenzhen University, Shenzhen 518060, China
[b] Beijing Key Laboratory of Indoor Air Quality Evaluation and Control, Department of Building Science, School of Architecture, Tsinghua University, Beijing 100084, China
[c] Songshan Lake Materials Laboratory, Dongguan 523808, China
[d] Institute of Physics, Chinese Academy of Sciences, Beijing 100190, China
[e] College of Civil Engineering, Hunan University, Changsha 410082, China
[f] State Key Laboratory of Intelligent Geotechnics and Tunnelling, Shenzhen 518060, China
[g] Key Laboratory of Coastal Urban Resilient Infrastructures, Ministry of Education, Shenzhen University, Shenzhen 518060, China
[h] Key Laboratory of Eco Planning & Green Building, Ministry of Education, Tsinghua University, Beijing 100084, China

ARTICLE INFO

Article history:
Received 11 February 2023
Revised 4 December 2023
Accepted 18 January 2024
Available online 29 February 2024

Keywords:
Weather-responsive facades
Building energy efficiency
Dynamic photovoltaic integrated building envelopes (PVBEs)
Building-integrated photovoltaics (BIPVs)

ABSTRACT

Substantially glazed facades are extensively used in contemporary high-rise buildings to achieve attractive architectural aesthetics. Inherent conflicts exist among architectural aesthetics, building energy consumption, and solar energy harvesting for glazed facades. In this study, we addressed these conflicts by introducing a new dynamic and vertical photovoltaic integrated building envelope (dvPVBE) that offers extraordinary flexibility with weather-responsive slat angles and blind positions, superior architectural aesthetics, and notable energy-saving potential. Three hierarchical control strategies were proposed for different scenarios of the dvPVBE: power generation priority (PGP), natural daylight priority (NDP), and energy-saving priority (ESP). Moreover, the PGP and ESP strategies were further analyzed in the simulation of a dvPVBE. An office room integrated with a dvPVBE was modeled using EnergyPlus. The influence of the dvPVBE in improving the building energy efficiency and corresponding optimal slat angles was investigated under the PGP and ESP control strategies. The results indicate that the application of dvPVBEs in Beijing can provide up to 131% of the annual energy demand of office rooms and significantly increase the annual net energy output by at least 226% compared with static photovoltaic (PV) blinds. The concept of this novel dvPVBE offers a viable approach by which the thermal load, daylight penetration, and energy generation can be effectively regulated.

1. Introduction

The building and construction sector accounted for 36% and 37% of the global energy demand and energy-related CO_2 emissions in 2020, respectively [1]. This issue is particularly pronounced in high-rise buildings with substantially glazed facades, which are recognized as the least energy-efficient building components [2,3]. This inefficiency can primarily be attributed to the substantial solar thermal gains or losses facilitated by glass curtain walls [4]. Highly glazed buildings consume significantly more energy than typical buildings [5]. Retrofitting building envelopes, particularly by incorporating shading devices, has positive effects on indoor thermal comfort, energy savings, and daylight glare control [6], making them crucial for enhancing the energy efficiency of buildings [7–9]. However, traditional shading devices result in a significant waste of solar energy through reflection [10]. The integration of area shading devices with photovoltaics (PVs), known as photovoltaic integrated building envelopes (PVBEs), constitutes a promising aspect of building-integrated photovoltaics (BIPVs) [11].

PVBEs are vital in passively reducing heating, ventilation, and air conditioning (HVAC) loads and positively converting solar energy incident on facades into electrical power, particularly in urban cities with abundant high-rise buildings [12,13]. Kant et al. [14] developed a comprehensive numerical study to simulate the effects of different PVBE design parameters but neglected the interactions with building thermal zones. Mandalaki et al. [10]

* Corresponding authors.
E-mail addresses: jqpeng@hnu.edu.cn (J. Peng), mojinhan@szu.edu.cn (J. Mo).

https://doi.org/10.1016/j.eng.2024.01.014

studied 13 types of fixed shading devices and showed that the electricity production of all shading devices with integrated south-facing PV was sufficient to support at least the lighting load of the reference office. Most reported PVBEs employ PV panels, blinds, and louvers with fixed inclined angles, that is, static PVBEs [15,16]. However, static PVBEs lack adjustability to enhance the visual comfort of occupants and are unresponsive to unpredictable weather conditions and seasonal changes. For instance, a static PVBE may work well on sunny days in the summer by reducing the cooling load and harvesting solar radiation for power generation, but it may increase the heating and artificial lighting loads on cloudy days in the winter. Long et al. [17] simulated the energy consumption and power generation of a fixed overhang integrated with PV panels in a student apartment in Changchun, China. The results indicated that the annual heating load surprisingly increased by more than 30% compared with the case without a shading system. Thus, static PV panels, blinds, and louvers cannot maximize the usage of incident solar radiation at all times because the incident angle of sunlight and other environmental characteristics change consistently throughout a day [18].

Recently, highly dynamic and weather-responsive PVBEs have been studied to further improve building energy efficiency. Mohtashami et al. [19] reviewed the technologies and requirements for a dynamic PVBE design and contributed to the development of dynamic PVBEs. Rotas et al. [20] assessed the annual energy performance improvement of buildings retrofitted with dynamic PVBEs and demonstrated considerable energy-saving potential. Abdullah et al. [21] presented a dual-axis solar-tracking shading device integrated with solar cells and emphasized the high energy performance in terms of the reduction of total energy consumption. Svetozarevic et al. [22] developed a dynamic PV module that actively modulated solar radiation and covered 115% of the net energy demand of an office. Paydar [23] designed an optimal movable inclined PV panel to effectively reduce the thermal load compared with fixed modes. Krarti [24] proposed a new dynamic overhang design for residential buildings and evaluated its positive impact in various climates in the United States, suggesting that sliding–rotating PV overhangs could significantly decrease the heating and cooling loads and increase the power generation of housing units in the United States. Recently, significant efforts have been made to promote the development of dynamic PVBEs. However, most of the aforementioned dynamic PVBEs were not specifically designed for high-rise buildings featuring large glazed facades. For example, the movable PV shading devices proposed by Paydar [23] and Krarti [24] require an additional external wall area to accommodate device repositioning, which poses challenges in applications involving highly glazed facades owing to the limited availability of the wall area. These nonretractable shading devices with large areas may adversely affect architectural aesthetics. Additionally, the dynamically adjustable PV panel arrays proposed by Abdullah et al. [21] and Svetozarevic et al. [22] have versatile mechanical structures for solar tracking, enabling excellent solar energy harvesting. However, relatively complex structures are not suitable for high-rise buildings because of their weak windproofing characteristics, which prevent their large-scale application in cities. Consequently, the development of simple, flexible, and intelligent PV shading devices continues to present significant challenges.

In this study, we propose a new type of dynamic and vertical photovoltaic integrated building envelope (dvPVBE) that achieves the fundamental functions of traditional PVBEs, responds to weather changes, and mitigates the impact on architectural aesthetics. Specifically, the dvPVBE is derived from a motorized PV blind and features a modern design, a compact structure, and the ability to flexibly adjust the slat angle and blind position. By incorporating adjustable slats and dynamic blind positions, the dvPVBE enhances thermal and visual comfort while also enabling *in situ* PV power generation under various weather conditions. In contrast to existing PVBE systems that automatically track the sun and generate electricity, the novel dvPVBE system provides greater flexibility in responding to weather changes and can reduce the overall energy consumption of buildings. Based on various scenarios, three control strategies for the dvPVBE are proposed, two of which are further explored with a simulation. Additionally, the potential of the adjustable slat angles of the dvPVBE to enhance energy performance was investigated through simulations using EnergyPlus, and a general method for solving the daily and annual optimal slat angles of the dvPVBE is proposed. These findings indicate that the dvPVBE has a positive impact on improving the energy efficiency of buildings.

2. dvPVBE

2.1. Design of the dvPVBE

The proposed dvPVBE was integrally assembled with highly glazed facades as a tight external layer of windows (Fig. 1(a)). The main body of the dvPVBE, including the frame structure and blind slats, is made of an aluminum alloy for light weight and superior strength to withstand severe weather. The slats integrated with the solar cells were dynamically motorized using a motor controller hidden in the top-frame structure. Moreover, compact, adjustable, and retractable slats mitigate negative impacts on architectural aesthetics.

Unlike traditional static external blinds, the slats of the dvPVBE can stop at any height of the frame and rotate between 0° and 90° via the precise stroke control of the motor. The video of the prototype presented in Vedio S1 in Appendix A demonstrates the multiple functions of the motorized blind and its actual operation. The mechanical structure of the prototype was derived from an existing motorized blind vehicle developed by a Chinese company. The blinds can be deployed partially or fully. When the blinds were stable, the slat angles were adjustable and could be flipped from 0° to 90°, corresponding to the vertical and horizontal positions of the slats. The aforementioned controls can be realized through wireless remote and computer controls. Thus, both the blind area exposed to solar radiation and the slat angle can be adjusted independently and intelligently to mitigate the external impacts of real-time weather conditions on indoor environments. The dvPVBE also allows for effective monitoring and maintenance management through the integration of sensors into the frame structure, including the monitoring of key factors such as temperature, wind speed, incident solar radiation, and power generation.

The numerous functions of the weather-responsive dvPVBE can be summarized as killing three birds with one stone: extraordinary flexibility with weather-responsive slat angles and blind positions, superior architectural aesthetics, and notable energy-saving potential.

(1) **Extraordinary flexibility with weather-responsive slat angles and blind positions.** As depicted in Figs. 1(b)–(e), the adjustable slat angle and blind position enable a wide range of dynamic actions that provide various combinations to respond to weather changes and the requirements of the occupants.

(2) **Superior external and internal architectural aesthetics.** The dvPVBE is tightly integrated into building facades, featuring a modern design, metallic appearance, and compact structure (Fig. 1(a)). With flexible slats, the dvPVBE creates an unobstructed and adjustable visual experience for pedestrians and occupants.

(3) **Notable energy-saving potential.** Integrated with solar cells, the dvPVBE can efficiently modulate the solar energy on the vertical facades of buildings. The slat angle can be adjusted

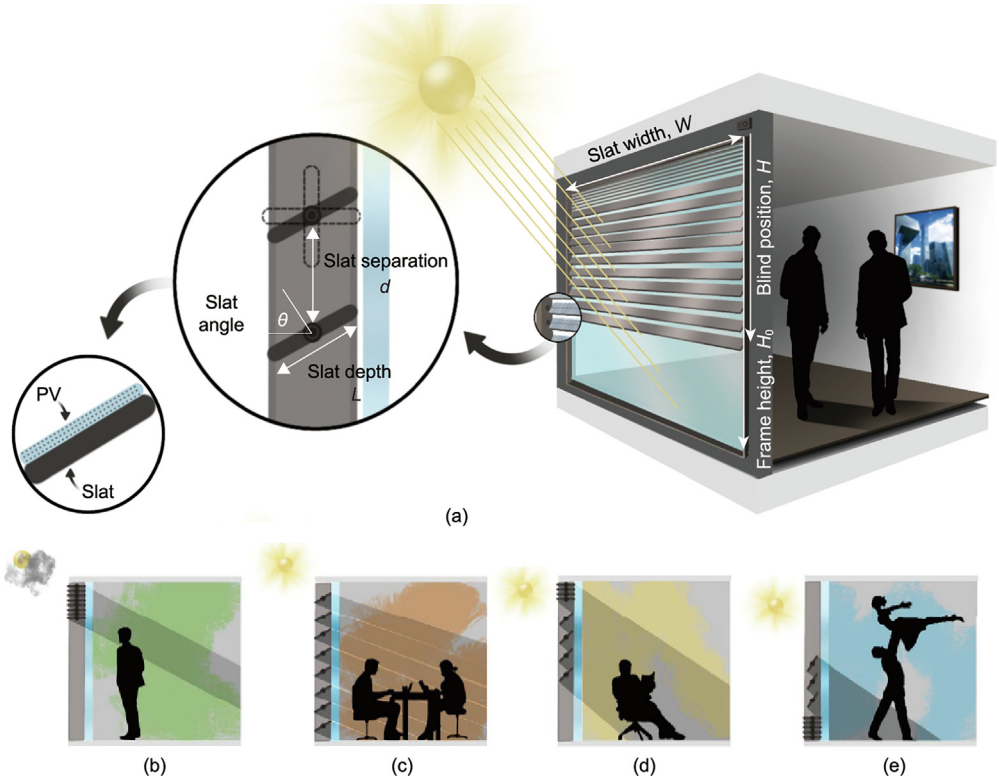

Fig. 1. Working principle and use cases of the weather-responsive dvPVBE. (a) The dvPVBE can effectively modulate solar radiation through the flexible control of the motorized slats. (b) On cloudy days, the slats are entirely retracted back to the top, providing sufficient daylight and an unobstructed view for occupants. (c) In the daytime of summer, the slats can be fully deployed to block direct sunlight from entering the room and convert solar energy into electricity. (d) In spring and autumn, the slats may be partially deployed to balance power generation and daylight penetration. (e) In winter, the slats can be partially retracted back to the bottom, allowing solar radiation to penetrate into the room while ensuring a good view from the top. More information can be found in Section S1 in Appendix A.

with the changing position of the sun to maximizing the incident solar radiation on the solar cells. Furthermore, the dvPVBE can reduce both the cooling load by blocking direct solar radiation in the summer (Fig. 1(c)) and the heating load by increasing the solar heat gains in the winter (Fig. 1(e)). The dvPVBE can also lower the lighting load through sufficient daylight penetration.

2.2. Control strategies of the dvPVBE

The structure parameters of the dvPVBE include the slat width (W), depth (L), separation (d), angle (θ), and blind position (H, the distance from the top frame to the bottom slat), as shown in Fig. 1(a). Typically, the slat width, depth, and separation are constant and determined at the design stage based on the window size [25]. This study analyzes the control of the slat angle and blind position and uses simulations to investigate the impact of the adjustable slat angles of the dvPVBE in enhancing building energy efficiency.

dvPVBE has two modes: manual and automatic. The manual mode is controlled by indoor occupants. For example, occupants can lift (Fig. 1(b)) or lower the blind (Fig. 1(d)) to improve the view from the inside. The automatic mode is programmed to dynamically control the blind position and slat angle based on weather conditions and the requirements of the occupants.

Fig. 2 illustrates three hierarchical control strategies of the dvPVBE in the automatic mode: power generation priority (PGP), energy-saving priority (ESP), and natural daylight priority (NDP). Four types of sensors were adopted for the control system: a pyranometer for measuring incident solar radiation on facades, an infrared sensor for monitoring indoor occupants, an illuminometer for measuring indoor illumination, and power meters for measuring the real-time electrical power consumption and generation. The control loop is executed at specific time intervals.

(1) **Strategy of PGP**. This strategy is adopted during non-working hours or when the room is unoccupied. This strategy adjusts the blind position H and the slat angle θ to maximize the incident solar radiation on the slats for PV power generation. First, the blind is fully deployed. That is, the blind position H equals H_0 (H_0 is the frame height, that is, the distance from the top to the bottom of the frame structure, as shown in Fig. 1(a)). The slat angle θ is then adjusted until the optimal angle for maximizing power generation (θ_p) is reached. Finally, the optimal angle θ_p is recorded and executed. Based on the results of previous studies, θ_p generally corresponds to the solar altitude angle and is set orthogonally to the solar profile angle without considering module self-shading [26,27].

(2) **Strategy of NDP**. This strategy aims to sufficiently utilize natural daylight to improve indoor illumination when a room is occupied. The specific implementation steps are as follows. First, H is set as H_0, and θ is set to the optimal angle θ_p, as mentioned in the PGP strategy. The indoor illuminance I is then measured and compared with the indoor set value I_0. If I is greater than or equal to I_0 and less than 2000 lx, the current state of H and θ will be retained. If I is greater than or equal to 2000 lx, θ will be slightly lessened by a small interval of $\Delta\theta$ until I is less than 2000 lx. If I is less than I_0, θ will be slightly enlarged by $\Delta\theta$ until I exceeds I_0. If I is still less than I_0, H will be lifted slightly by a small interval of ΔH until I exceeds I_0. Ultimately, indoor illumination is fulfilled by the sufficient utilization of natural daylight, and the lighting load is incidentally reduced.

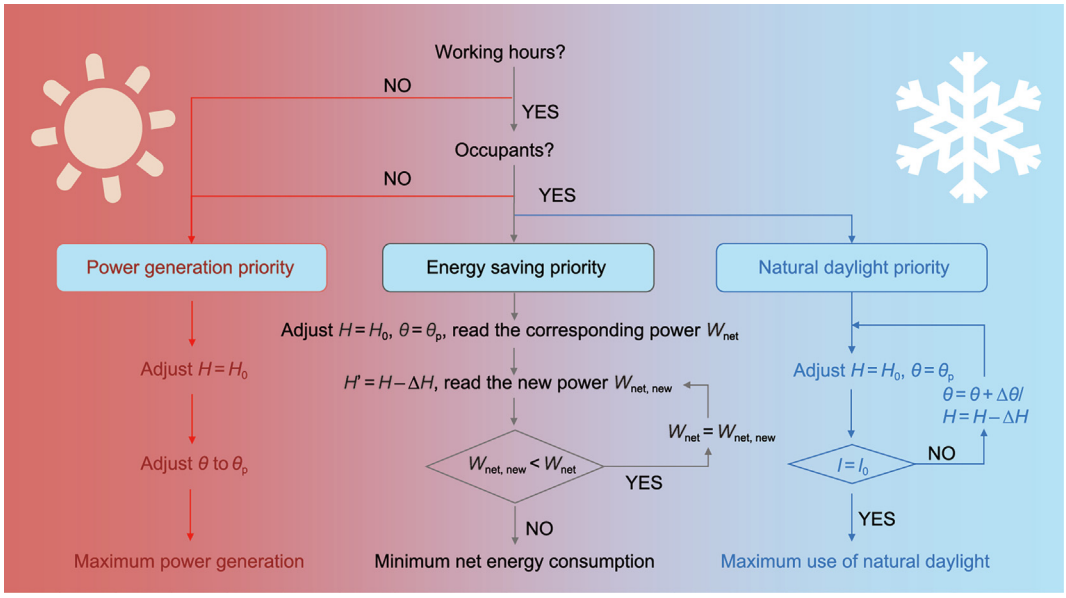

Fig. 2. Workflow of three control strategies corresponding to different scenarios. H_0 is the frame height, that is, the distance from the top to the bottom of the frame structure. θ_p is the optimal slat angle for maximum power generation. W_{net} is the net power corresponding to the blind position. ΔH is the distance step for the blind position adjustment. $\Delta\theta$ is the angle step for the slat angle adjustment. I is the indoor illuminance. I_0 is the set value of indoor illumination. In this study, I_0 was set as 300 lx as the daylight illuminance reference.

(3) **Strategy of ESP**. This strategy is designed to minimize the net energy consumption of the room. Thus, the energy consumption of the HVAC and lighting systems as well as the PV power generation are considered. The influences of building thermal inertia, indoor thermal mass diffusion, heat transmission, and the distribution efficiency of air conditioning systems lead to a significant lag in the performance of air conditioning systems [28–30]. Owing to this inherent lag and the resulting difficulty in system control for heating and cooling, the precise optimization of real-time net energy consumption is difficult to implement. The control loop illustrated in Fig. 2 provides an approximate but practical method. First, H is set as H_0, and θ is set to the optimal angle θ_p. Second, the net power consumption of the room, W_{net}, is calculated using Eq. (1). Third, H will be slightly lifted by a small interval of ΔH to obtain a new $W_{net,new}$ at the new H. If $W_{net,new}$ is less than W_{net}, the third step will be repeated until $W_{net,new}$ is greater than W_{net}. If $W_{net,new}$ is greater than W_{net}, the slats will revert to the previous state. This operational strategy can effectively reduce the net energy consumption.

$$W_{net} = W_{HVAC} + W_{light} - W_{PV} \quad (1)$$

where W_{HVAC} is the instantaneous power consumption of the HVAC system, W_{light} is the instantaneous power consumption of the lighting system, W_{PV} is the instantaneous power generation of the PV array, and W_{net} is the net power in the room. The instantaneous power was measured using a power meter.

2.3. Simulation setup

In the simulation, a model was built to investigate the energy performance and optimal configuration of the dvPVBE. A 24-story office building located in Beijing, China, was created using the three-dimensional modeling software SketchUp, as shown in Fig. S1 of Section S2 in Appendix A. It is assumed that there are no additional high-rise buildings surrounding the office building. Thus, the shading and reflection caused by surrounding buildings are ignored in this study. A south-facing room with a size of 5 m × 5 m × 3 m that is located on the south-facing facade of the building was chosen as the representative room. Except for the glazed facade exposed to the external environment, all other surfaces (walls, floors, and ceilings) exposed to the indoor environment were considered adiabatic by assuming adjacent rooms at the same indoor temperature [31]. The glazed facade is 4.8 m × 2.184 m in size, resulting in a window-to-wall ratio of 70%. Specifically, the glazed facade is equipped with a double-pane window with a heat transfer coefficient (U-factor) of 1.8 W·(m^2·K)$^{-1}$ and a solar heat gain coefficient of 0.4. The heat transfer coefficient of the exterior walls is 0.485 W·(m^2·K)$^{-1}$. All parameter settings of the building envelope complied with the China Design Standard for Energy Efficiency in Public Buildings (GB 50189—2015) [32]. Table 1 [33,34] summarizes key information regarding the building models. The availability of an HVAC system depends on the climate in Beijing. Specifically, the cooling mode of the HVAC system is activated from May to September to ensure that the indoor temperature remains below 26 °C. The heating mode is activated from November to February to ensure that the indoor temperature remains above 18 °C. In addition, the HVAC system starts one hour before working hours to ensure a comfortable indoor thermal environment for employees coming to work at 8 a.m. Therefore, the HVAC system was activated from 7 a.m. to 6 p.m. on weekdays.

The dvPVBE mounted on the exterior surface of the glazed facade consisted of 24 slats integrated with solar cells, as shown in Fig. S1. Each slat consisted of 26 solar cells, manufactured by Jinko Solar (China) in series. The ratio of slat separation (d) to slat depth (L) was set to 1 (d/L = 1) to enhance the indoor visual comfort. Detailed information on the slats and solar cells is listed in Table 1.

The energy performance of the building room was simulated using open-source whole-building energy modeling software (EnergyPlus, version 9.6), which can simulate transient heat conduction, daylighting controls, and onsite PV power generation [35,36]. To investigate the overall energy performance of the dvPVBE, several submodels were employed in EnergyPlus, including heat balance, daylighting, and power generation models [37]. The heat balance model in EnergyPlus was adopted to simulate

Table 1
Specifications for the building energy performance modeling.

Parameter			Value
Building model		Total floor area	25 m^2
		Fresh air supply rate per person	30 m^3·(h·person)$^{-1}$
		Number of people	4
		People per floor area	0.16 person·m^{-2}
		Lighting power per floor area	9 W·m^{-2}
		Other electric equipment power per floor area	12 W·m^{-2}
		Working hours of occupants	8 a.m. to 6 p.m. (weekdays)
		HVAC system	Packaged terminal heat pump (PTHP)
		Heating set point	18 °C
		Cooling set point	26 °C
		Performance coefficient of heat pump[a]	Summer: 3.0; winter: 2.5
Blind slat and solar cell	Slat	Slat width	4.80 m
		Slat depth	0.091 m
		Slat separation	0.091 m
		Slat angle	Dynamic
		Number of slats	24
	Solar cell	Manufacturer	Jinko Solar (China)
		Material	Monocrystalline silicon
		Dimensions (single solar cell)	0.182 m × 0.091 m
		Nominal efficiency	21.32%
		Nominal operating cell temperature (NOCT)	45 °C

[a] Performance parameters for the summer and winter were taken from the studies by Boyano et al. [33] and Wei et al. [34], respectively.

the heat transfer and energy flows within buildings and to calculate the heating and cooling loads of the buildings [38]. Conduction transfer functions, which are well-established and have been extensively validated within the building energy analysis field, were chosen as the algorithms. The daylighting model was used to simulate daylighting performance at different slat angles and identify their influence on the lighting load. The daylight illuminance reference point was set as 300 lx at 0.75 m above the floor in the middle of the room, and the continuous dimming control of lighting was adopted. In this study, the equivalent one-diode model, known as the five-parameter model [39], was selected for the PV performance prediction simulation using equivalent circuits models derived from diodes.

For the control strategies of the dvPVBE, the PGP strategy was used during non-working hours, and the ESP strategy was used during working hours. The NDP strategy was greatly affected by occupant preferences and was therefore left for further analysis in future research. To further demonstrate the viability of the dvPVBE in enhancing building energy efficiency and conduct a fair comparison with static PV blinds, the simulation primarily focused on evaluating the influence of adjustable slat angles on energy performance. Specifically, the blind position is set to H_0 in the following simulation, similar to the traditional static PV blinds used in previous studies [31,40].

The optimal slat angles for the dvPVBE were obtained using a combination of static PV blind cases. Nineteen static PV blind cases from 0° to 90° in increments of 5° were studied, and the optimal configuration of the dvPVBE was a combination of slat angles subject to the lowest net energy consumption constraint in the 19 static cases. The HVAC load, lighting load, and PV generation varied in different cases, collectively affecting the net energy consumption of the room. Compared with the HVAC load, lighting load, and power generation, the energy consumption of the motors and controllers in the dvPVBE system is negligible, owing to their intermittent operation and low nominal power. Detailed simulation data for the 19 static PV blind cases and the dvPVBE throughout the year are presented in Section S3 in Appendix A. The method used to determine the optimal configuration of the dvPVBE is applicable to various environmental conditions. In this study, Beijing was selected as an example to assess the energy performance of the dvPVBE.

3. Results and discussion

3.1. Optimal configurations of the dvPVBE on typical seasonal days in Beijing

Four typical days around the vernal equinox, summer solstice, autumnal equinox, and winter solstice were selected to analyze the influence of seasonal changes on the energy performance and optimal configurations of the dvPVBE in detail and provide references for year-round optimization. The vernal equinox is the moment when the sun appears to cross the celestial equator and head northward. The summer solstice occurs when the sun is at its highest position in the Northern Hemisphere. The autumnal equinox is the moment when the sun appears to cross the celestial equator and head southward. The winter solstice is when the sun is at its lowest daily maximum elevation in the sky in the Northern Hemisphere. The four selected days were sunny weekdays with high solar radiation. More information and definitions on the four selected days can be found in Table S1 of Section S2 in Appendix A. Fig. 3 shows the hourly HVAC loads, lighting loads, and PV generation of the building rooms in Beijing, along with the optimal hourly slat angles. The high consumption before 8 a.m. was caused by the starting load of the HVAC system, as the HVAC system starts one hour before working hours. As the energy consumption of the other electrical equipment remains constant and does not affect the optimal configuration, it is not discussed herein.

Figs. 3(a) and (c) show that the hourly energy generation of PV (blue bars) was much greater than the hourly energy consumption of the HVAC and lighting (gray bars) between 8 a.m. and 4 p.m. on the vernal and autumnal equinoxes, respectively. This indicates that the solar cells on the dvPVBE generated more electricity than the energy demand of the room for most of the day. Fig. 3(b) shows that this trend slows down and even appears inversely during the summer solstice, owing to the rapidly rising cooling loads. Furthermore, benefiting from the lower position of the sun, PV generation was still dominant in the afternoon and accounted for over 70% of the energy consumption throughout the day during the winter solstice, as shown in Fig. 3(d).

The optimal hourly slat angles were determined based on the combined effects of the HVAC, lighting, and PV systems. Figs. 3(a) and (c) show that when the sun was directly overhead at the equator during the vernal and autumnal equinoxes, the hourly slat angles varied from 40° to 90° and were almost stable at approximately 45° during the daytime. Owing to the mild weather during the vernal equinox, the HVAC load is much lower than the PV power generation and can be negligible. For instance, Fig. 3(a) shows that from 11 a.m. to 12 a.m., the PV power generation was more than 1.08 kW·h, almost twice the entire day's HVAC and lighting loads. Therefore, the slat angles were optimized based on the lighting load and PV power generation. Regarding the lighting load, natural daylight can provide sufficient illumination at 45° or larger slat angles to meet the illumination requirements of the indoor environment. Owing to sufficient daylight penetration, the lighting system of the room was dimmed to lower the lighting load. The PV power generation gradually decreases as the slat angle increases, and this is affected by the solar radiation incident on the slats and module self-shading, which is detrimental to the energy

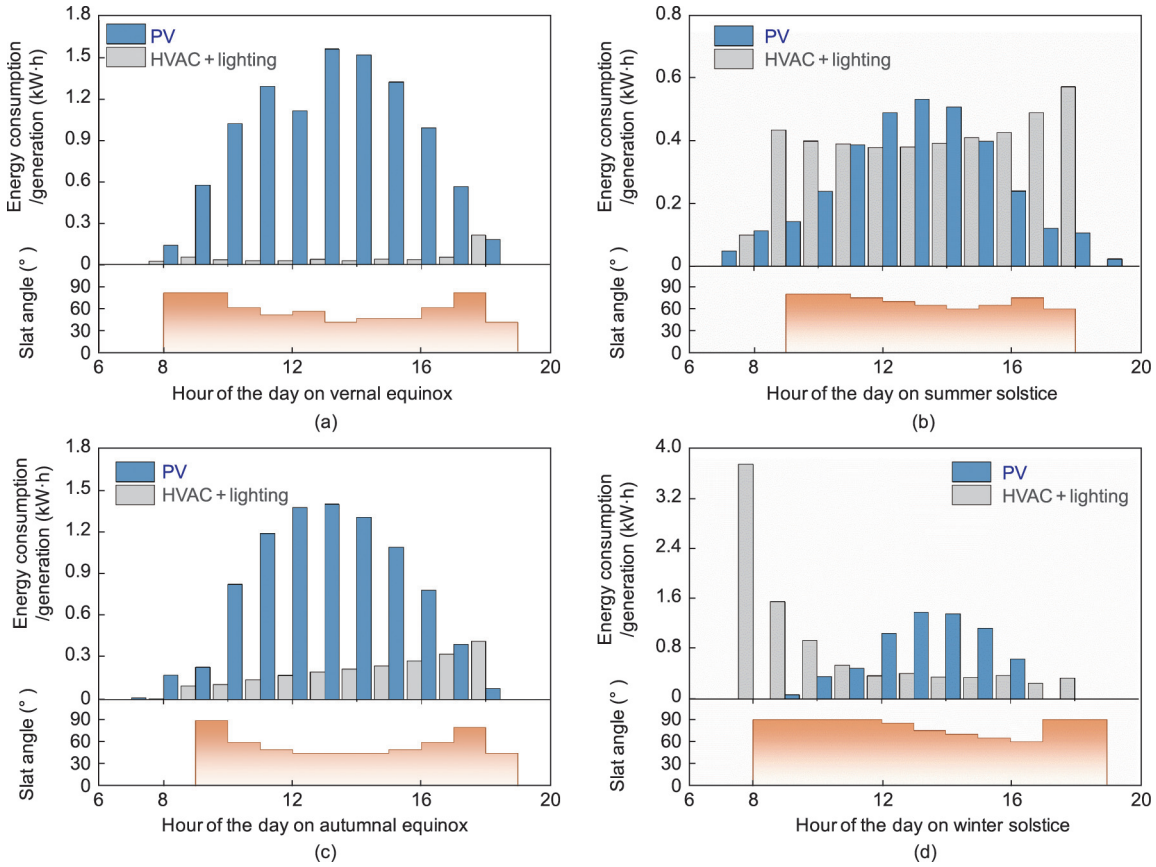

Fig. 3. Optimal configurations and corresponding energy performance of the dvPVBE for selected typical seasonal days in Beijing: (a) vernal equinox, (b) summer solstice, (c) autumnal equinox, and (d) winter solstice.

performance of the PV arrays [41]. Hence, there is a tradeoff between lighting and PV. In the early morning, when the solar radiation is low, the slat angles are adjusted to nearly 90° to minimize the lighting load. Conversely, when the solar radiation is high in the afternoon, the slat angles are optimized to approximately 45° to maximize the utilization of both natural light and solar energy. The same approach was applied during the autumnal equinox.

During the summer solstice, the cooling load experiences a significant increase, but it is not largely affected by changes in the slat angle, owing to the close arrangement of the slats. For instance, between 1 p.m. and 2 p.m., the cooling load increased by less than 0.03 kW•h when the slat angle was set at 90°, compared with 0°. In contrast, the lighting load was reduced by more than 0.2 kW•h to just 10% of the load at 0°. Simultaneously, the effect of the slat angle change on PV power generation is not evident, owing to high module self-shading. Consequently, the optimization of the slat angles primarily focused on reducing the lighting load with an optimal angle of approximately 70° to allow sufficient daylight penetration, as shown in Fig. 3(b).

During the winter solstice, the slats were adjusted to 90° to allow maximum sunlight to enter the room, thereby reducing the need for heating and lighting. However, slats at 0° are the most favorable for solar energy utilization because of the low position of the sun and low module self-shading. Therefore, from 12 a.m. to 4 p.m., the slat angles are optimized at approximately 65°, which is a compromise angle for utilizing abundant solar energy, and the dvPVBE generates more than 4.44 kW•h of clean electricity. For the rest of the day, the slat angles were close to 90° to minimize the heating and lighting loads, as shown in Fig. 3(d).

Table 2 summarizes the energy performance of the dvPVBE and five static PV blind cases on four selected days in Beijing. If the net energy consumption is negative, the PV power generation is greater than the HVAC and lighting loads, and the absolute value of the net energy consumption represents the net energy output. The results indicate that the energy performance of static PV blinds varies significantly with the season. For example, the 90° angle case performs best during the winter solstice but worst during the summer solstice because of the decrease in the energy-saving potential of the HVAC and lighting loads. Nevertheless, the dvPVBE can balance the HVAC and lighting loads with PV generation, achieving an increase in the total net energy output of at least 34.7%. The results in Table 2 show that the dvPVBE has advantages in temperate and hot climates.

3.2. Optimal annual configurations of the dvPVBE in Beijing

Based on the results presented in Section S3 in Appendix A, Fig. 4 presents the optimal hourly slat angles of the dvPVBE over the entire year under PGP and ESP control through a heat map for visualization [42]. To better present the slat angle variation in different months and weaken the influence of meteorological fluctuations, the median values of the slat angles at the same hour of the day in each month are shown in the heat map. Additionally, the slat angles are adjusted from 7 a.m. to 6 p.m. During other periods, the slat angle is fixed at 0° to protect indoor privacy during the absence of energy consumption and power generation.

Fig. 4 shows that the slat angles were optimized at 45°–60° for most of the year to minimize the net energy consumption. During the early morning hours, large slat angles of approximately 90° are adopted to reduce the lighting load. Additionally, the variation in the slat angle shows seasonal characteristics. When the subsolar point migrates northward after the winter solstice, the medium slat angles dominate with the gradual prominence of PV power

Table 2
Energy performance of the dvPVBE and static PV blinds in Beijing (unit: kW·h).

Specific day	Indicator	dvPVBE	Static PV blind with fixed slat angle				
			0°	30°	45°	60°	90°
Vernal equinox	HVAC and lighting loads	0.56	2.44	1.55	0.99	0.71	0.44
	PV generation	10.17	11.04	10.63	10.35	10.06	9.26
	Net energy consumption	−9.61	−8.60	−9.08	−9.36	−9.35	−8.82
Summer solstice	HVAC and lighting loads	4.36	5.73	5.22	4.89	4.60	4.46
	PV generation	3.34	4.28	3.82	3.52	3.26	2.75
	Net energy consumption	1.02	1.45	1.40	1.37	1.34	1.71
Autumnal equinox	HVAC and lighting loads	2.19	3.87	2.97	2.45	2.30	2.40
	PV generation	8.88	9.66	9.28	9.03	8.75	8.14
	Net energy consumption	−6.68	−5.79	−6.31	−6.57	−6.45	−5.74
Winter solstice	HVAC and lighting loads	9.17	23.26	23.15	22.08	17.97	7.88
	PV generation	6.43	10.58	10.33	10.02	8.87	4.32
	Net energy consumption	2.74	12.69	12.83	12.06	9.10	3.56
Total	Net energy consumption	−12.53	−0.25	−1.16	−2.50	−5.36	−9.29

Negative values of net energy consumption indicate that the energy production is greater than the energy consumption.

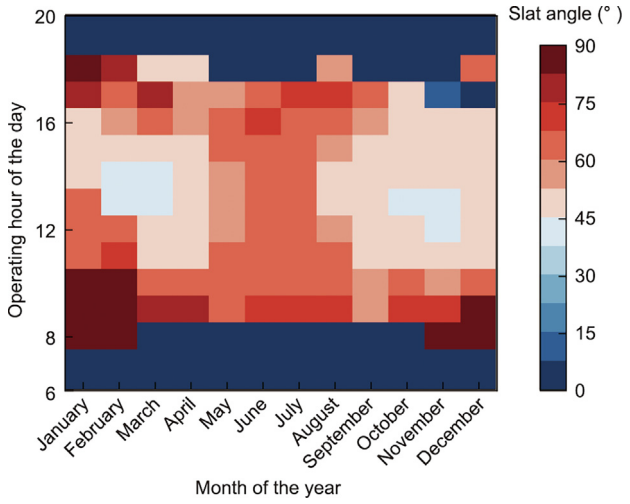

Fig. 4. Heat map details the median of the optimal slat angles in each month throughout the year in Beijing. Small slat angles correspond to vertical positions of the slats, and large slat angles correspond to horizontal positions.

generation. For instance, the hourly slat angles in March were stable at approximately 45° from 10 a.m. to 3 p.m., which is consistent with the optimal schedule for the vernal equinox. Moreover, from May to August, the slat angles gradually increased to 65° during the daytime, effectively reducing the lighting load while ensuring adequate PV power generation. When the subsolar point migrates southward before the winter solstice, the slat angles are optimized to 45° to utilize natural daylight and solar energy efficiently. From November to February, the optimal slat angle was increased to 60° to ensure sufficient sunlight in the room, thereby reducing the heating load.

Fig. 5 presents a comparison of the annual energy performance of the dvPVBE and static PV blinds in Beijing. This investigation explores PV generation, HVAC and lighting loads, other electrical equipment ("Others" in Fig. 5), and net energy output ("Total" in Fig. 5). In all cases, the annual energy consumption of the other electrical equipment remained constant at 783 kW·h per year. The net energy output of the static PV blinds exhibited an initial increase, followed by a decrease, with an increase in the slat angle. Furthermore, the cases featuring slat angles of 45°–60° showed the best performance in increasing the net energy output, which agrees with the results reported by Li et al. [43]. Among the five static cases, the 45° angle case had the largest annual net energy output of 153 kW·h, benefiting from a well-balanced combination of HVAC, lighting, and PV.

Nevertheless, dvPVBE still exhibits a considerable advantage over the 45° angle case, with a relative 32.5% drop in HVAC and lighting loads and a modest 2.4% drop in PV generation. The PV power generation of the dvPVBE can cover up to 131% of the annual energy demand of the office. The dvPVBE can benefit from daily, seasonal, and annual external environmental changes to the greatest extent through dynamic adjustment. Within one day, the dvPVBE can reduce the lighting load by increasing the slat angle during the early morning hours. In spring and autumn, the dvPVBE can adjust the slat angle to approximately 45° to take full advantage of natural light and solar energy. Throughout the year, the dvPVBE can respond dynamically to the changing external environment to achieve the best balance among HVAC, lighting, and PV. Overall, the annual net energy output of the dvPVBE increased by at least 226%, showing significant advantages for clean energy gains.

In addition, dvPVBE has positive economic and environmental benefits. Excess PV energy is injected into the electric grid to provide additional income while simultaneously mitigating carbon emissions. To standardize the results, we normalized the net energy output, PV energy income, and carbon emissions based on the net heated and cooled areas of the building room (25.0 m^2). Fig. 6 [44] shows that the dvPVBE can lead to a relative annual increase of 227% in PV income and carbon emission reduction compared with the 45° angle case.

3.3. Limitations of the study

In this study, the concept of a dvPVBE was proposed, and its significant energy-saving potential over static PV blinds was demonstrated. However, this study has several limitations.

The daily and annual optimal dynamic configurations of the dvPVBE were obtained using a combination of static configurations consisting of 19 static PV blind cases. This is a simple and general method for solving for the optimal configuration, but it may not be sufficient for operation. In actual operation, the dvPVBE must be adjusted in time to respond to weather and indoor changes. Therefore, the real dynamism of the dvPVBE system would be based on real-time sensing data. In future studies, a sensing-based machine learning control method may realize the real dynamism of the dvPVBE system.

In the simulation, the blind position was fixed, and its impact on energy performance was not investigated. In addition, shading from surrounding buildings and the energy performance of the dvPVBE under different environmental conditions were not considered. Additional dynamic actions of the blind position, surrounding buildings, and environmental conditions will be considered in future studies.

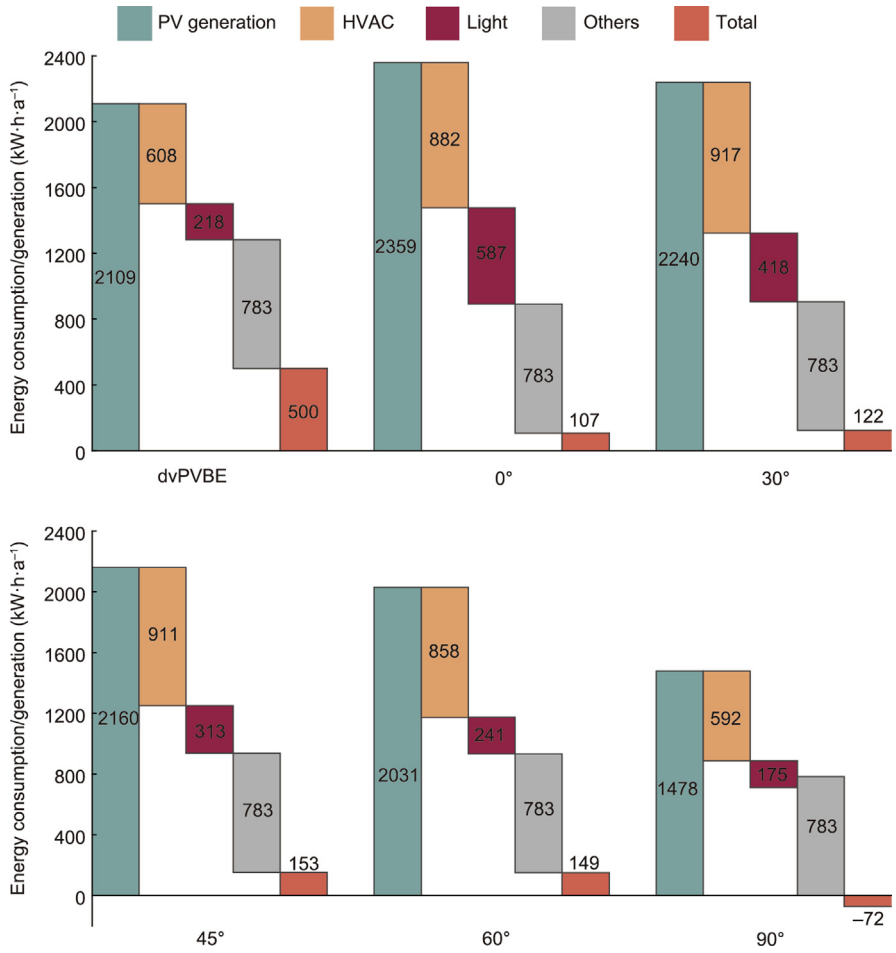

Fig. 5. Comparison of annual energy performance between the dvPVBE and traditional static PV blinds in Beijing.

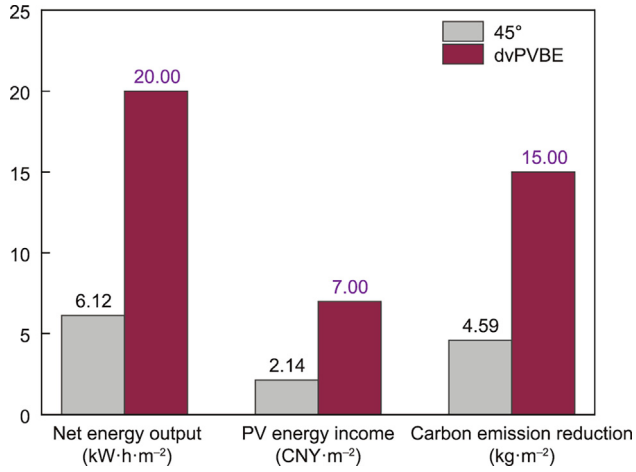

Fig. 6. Comparison of annual net energy output, PV energy income, and carbon emission reduction per floor area between the dvPVBE and static 45° angle case in Beijing. The average solar PV feed-in tariff is ~0.35 CNY·(kW·h)$^{-1}$ in China. The carbon emissions per unit of electricity (generated by conventional fuels) are estimated to be ~750 g CO_2 per kilowatt-hour by the International Energy Agency [44].

Several factors can be studied in the future, including slat depth, slat separation, dvPVBE orientation, and PV efficiency. The PV modules used in this study were monocrystalline silicon cells with an efficiency of 21.32%, which could be further improved. Driven by significant advances in solar cell materials, silicon solar cells have recently achieved a record efficiency of 26.7% [45], whereas thin-film solar cells such as Cu(In,Ga)Se_2 reached an efficiency of 23.3% [46] and emerging PV technologies, such as perovskite cells, have reached 25.6% [47]. The high efficiency of solar cells is a promising prospect for dvPVBE applications. Furthermore, the utilization of the electricity generated by the PV system can be improved through the integration of an energy storage system within the building, which could enhance the energy performance of the dvPVBE. The environmental and cost impacts of dvPVBE are also crucial and may be studied through a life cycle assessment (LCA) and life cycle cost (LCC) analysis in future work [48]. The LCA and LCC analyses will help evaluate the overall environmental implications and economic considerations associated with the implementation of dvPVBE.

Moreover, the critical advantage of the dvPVBE is that it allows occupants in high-rise buildings to obtain satisfactory window views and enjoy natural daylight. Thus, the indoor light environment, work ability, job satisfaction, and occupant well-being could be further evaluated. The qualitative requirements of occupants for glare control, better outdoor views, and privacy protection should be considered comprehensively in future studies.

4. Conclusions

The development of dvPVBEs holds great potential for high-rise buildings with substantially glazed facades in modern cities. In this paper, we propose a new type of dvPVBE derived from motorized

blinds that exhibits extraordinary flexibility, superior architectural aesthetics, and notable energy-saving potential. The results showed the excellent energy performance of an office room integrated with the dvPVBE in Beijing, providing valuable references for buildings facing similar conditions. The primary findings of this study are summarized as follows.

(1) The proposed dvPVBE system exhibited excellent flexibility with an adjustable slat angle and blind position, providing effective options for responding to weather changes. The simple and retractable structure of this system mitigates its negative impact on architectural aesthetics.

(2) Three operational control strategies are proposed for different scenarios: PGP, NDP, and ESP. A building model under PGP and ESP control was set up in EnergyPlus to simulate the energy performance of the dvPVBE in Beijing. To determine the daily and annual optimal configurations of the dvPVBE, a general method is introduced.

(3) The optimal configurations of the dvPVBE and a further explanation of the results are provided to guide dynamic control, considering the comprehensive influences of HVAC, lighting, and PV. For most of the daytime throughout the year in Beijing, 45°–60° slat angles are recommended to balance the utilization of natural light and solar energy. In the early morning, large slat angles are recommended to allow sufficient daylight penetration to lower the lighting load, particularly in the winter.

(4) The dvPVBE exhibited superior energy performance compared with the static PVBEs throughout the year. The application of the dvPVBE can cover up to 131% of the annual energy demand of an office room in Beijing and increase the annual net energy output by at least 226% compared with traditional static PV blinds, thereby promoting the development of net zero-energy buildings.

In conclusion, the proposed dvPVBE represents a promising application of BIPVs that offers significant opportunities to enhance the energy efficiency of high-rise buildings with large glazed facades. This study is expected to make a significant contribution to energy savings and decarbonization in the building sector through the effective regulation of the thermal load, daylight penetration, and energy generation.

Acknowledgment

The work was supported by the National Natural Science Foundation of China (52078269 and 52325801).

Compliance with ethics guidelines

Wuwei Zou, Yan Wang, Enze Tian, Jiaze Wei, Jinqing Peng, and Jinhan Mo declare that they have no conflict of interest or financial conflicts to disclose.

Appendix A. Supplementary data

Supplementary data to this article can be found online at https://doi.org/10.1016/j.eng.2024.01.014.

References

[1] Zhang S, Ma M, Xiang X, Cai W, Feng W, Ma Z. Potential to decarbonize the commercial building operation of the top two emitters by 2060. Resour Conserv Recycl 2022;185:106481.
[2] Ke Y, Chen J, Lin C, Wang S, Zhou Y, Yin J, et al. Smart windows: electro-, thermo-, mechano-, photochromics, and beyond. Adv Energy Mater 2019;9(39):1902066.
[3] Wang S, Jiang T, Meng Y, Yang R, Tan G, Long Y. Scalable thermochromic smart windows with passive radiative cooling regulation. Science 2021;374(6574):1501–4.
[4] Zhou Y, Wang S, Peng J, Tan Y, Li C, Boey FYC, et al. Liquid thermo-responsive smart window derived from hydrogel. Joule 2020;4(11):2458–74.
[5] Poirazis H, Blomsterberg Å, Wall M. Energy simulations for glazed office buildings in Sweden. Energy Build 2008;40(7):1161–70.
[6] Kirimtat A, Koyunbaba BK, Chatzikonstantinou I, Sariyildiz S. Review of simulation modeling for shading devices in buildings. Renew Sustainable Energy Rev 2016;53:23–49.
[7] Hawas A, Al-Habaibeh A. An innovative approach towards enhancing energy conservation in buildings via public engagement using DIY infrared thermography surveys. Energy Built Environ 2022;3(1):1–15.
[8] Chen B, Zhang M, Hou Y, Wang H, Zhang R, Fan Y, et al. Energy saving thermal adaptive liquid gating system. Innovation 2022;3(3):100231.
[9] Fan Y, Xia X. A multi-objective optimization model for energy-efficiency building envelope retrofitting plan with rooftop PV system installation and maintenance. Appl Energy 2017;189:327–35.
[10] Mandalaki M, Zervas K, Tsoutsos T, Vazakas A. Assessment of fixed shading devices with integrated PV for efficient energy use. Sol Energy 2012;86(9):2561–75.
[11] Skandalos N, Karamanis D. An optimization approach to photovoltaic building integration towards low energy buildings in different climate zones. Appl Energy 2021;295:117017.
[12] Zhang X, Lau SK, Lau SSY, Zhao Y. Photovoltaic integrated shading devices (PVSDs): a review. Sol Energy 2018;170:947–68.
[13] Taveres-Cachat E, Lobaccaro G, Goia F, Chaudhary G. A methodology to improve the performance of PV integrated shading devices using multi-objective optimization. Appl Energy 2019;247:731–44.
[14] Kant K, Pitchumani R, Shukla A, Sharma A. Analysis and design of air ventilated building integrated photovoltaic (BIPV) system incorporating phase change materials. Energy Convers Manage 2019;196:149–64.
[15] Mandalaki M, Tsoutsos T, Papamanolis N. Integrated PV in shading systems for Mediterranean countries: balance between energy production and visual comfort. Energy Build 2014;77:445–56.
[16] Hwang T, Kang S, Kim JT. Optimization of the building integrated photovoltaic system in office buildings—focus on the orientation, inclined angle and installed area. Energy Build 2012;46:92–104.
[17] Long W, Chen X, Ma Q, Wei X, Xi Q. An evaluation of the PV integrated dynamic overhangs based on parametric performance design method: a case study of a student apartment in China. Sustainability 2022;14(13):7808.
[18] Kirimtat A, Tasgetiren MF, Brida P, Krejcar O. Control of PV integrated shading devices in buildings: a review. Build Environ 2022;214:108961.
[19] Mohtashami N, Fuchs N, Fotopoulou M, Drosatos P, Streblow R, Osterhage T, et al. State of the art of technologies in adaptive dynamic building envelopes (ADBEs). Energies 2022;15(3):829.
[20] Rotas R, Fotopoulou M, Drosatos P, Rakopoulos D, Nikolopoulos N. Adaptive dynamic building envelopes with solar power components: annual performance assessment for two pilot sites. Energies 2023;16(5):2148.
[21] Abdullah HK, Alibaba HZ. Retrofits for energy efficient office buildings: integration of optimized photovoltaics in the form of responsive shading devices. Sustainability 2017;9(11):2096.
[22] Svetozarevic B, Begle M, Jayathissa P, Caranovic S, Shepherd RF, Nagy Z, et al. Dynamic photovoltaic building envelopes for adaptive energy and comfort management. Nat Energy 2019;4(8):671–82.
[23] Paydar MA. Optimum design of building integrated PV module as a movable shading device. Sustainable Cities Soc 2020;62:102368.
[24] Krarti M. Evaluation of PV integrated sliding–rotating overhangs for US apartment buildings. Appl Energy 2021;293:116942.
[25] Hu H, Xu W, Li A, Chu J, Lv Y. Sensitivity analysis and prediction of shading effect of external venetian blind for nearly zero-energy buildings in China. J Build Eng 2021;41:102401.
[26] Kim SH, Kim IT, Choi AS, Sung M. Evaluation of optimized PV power generation and electrical lighting energy savings from the PV blind-integrated daylight responsive dimming system using LED lighting. Sol Energy 2014;107:746–57.
[27] Hong S, Choi AS, Sung M. Development and verification of a slat control method for a bi-directional PV blind. Appl Energy 2017;206:1321–33.
[28] Verbeke S, Audenaert A. Thermal inertia in buildings: a review of impacts across climate and building use. Renewable Sustainable Energy Rev 2018;82(Pt 3):2300–18.
[29] Meng Y, Li T, Liu G, Xu S, Ji T. Real-time dynamic estimation of occupancy load and an air-conditioning predictive control method based on image information fusion. Build Environ 2020;173:106741.
[30] Li W, Yang L, Ji Y, Xu P. Estimating demand response potential under coupled thermal inertia of building and air-conditioning system. Energy Build 2019;182:19–29.
[31] Singh R, Lazarus IJ, Kishore VVN. Uncertainty and sensitivity analyses of energy and visual performances of office building with external venetian blind shading in hot-dry climate. Appl Energy 2016;184:155–70.
[32] Liang Y, Wu H, Huang G, Yang J, Wang H. Thermal performance and service life of vacuum insulation panels with aerogel composite cores. Energy Build 2017;154:606–17.
[33] Boyano A, Hernandez P, Wolf O. Energy demands and potential savings in European office buildings: case studies based on EnergyPlus simulations. Energy Build 2013;65:19–28.
[34] Wei W, Jin X, Dong Q, Ni L, Zhao S, Wang W, et al. Frosting performance variations of variable-frequency air source heat pump in different climatic regions. Appl Therm Eng 2023;219(Pt A):119356.
[35] Crawley DB, Lawrie LK, Winkelmann FC, Buhl WF, Huang YJ, Pedersen CO, et al. EnergyPlus: creating a new-generation building energy simulation program. Energy Build 2001;33(4):319–31.

[36] Lu W. Dynamic shading and glazing technologies: improve energy, visual, and thermal performance. Energy Built Environ 2024;5(2):211–29.
[37] Peng J, Curcija DC, Lu L, Selkowitz SE, Yang H, Zhang W. Numerical investigation of the energy saving potential of a semi-transparent photovoltaic double-skin facade in a cool-summer Mediterranean climate. Appl Energy 2016;165:345–56.
[38] Strand RK. Incorporating two-dimensional conduction modeling techniques into an energy simulation program: the EnergyPlus radiant system example. Energy Build 2022;274:112405.
[39] Saber EM, Lee SE, Manthapuri S, Yi W, Deb C. PV (photovoltaics) performance evaluation and simulation-based energy yield prediction for tropical buildings. Energy 2014;71:588–95.
[40] Huo H, Xu W, Li A, Lv Y, Liu C. Analysis and optimization of external venetian blind shading for nearly zero-energy buildings in different climate regions of China. Sol Energy 2021;223:54–71.
[41] Brecl K, Topič M. Self-shading losses of fixed free-standing PV arrays. Renewable Energy 2011;36(11):3211–6.
[42] Jayathissa P, Luzzatto M, Schmidli J, Hofer J, Nagy Z, Schlueter A. Optimising building net energy demand with dynamic BIPV shading. Appl Energy 2017;202:726–35.
[43] Li X, Peng J, Li N, Wu Y, Fang Y, Li T, et al. Optimal design of photovoltaic shading systems for multi-story buildings. J Cleaner Prod 2019;220:1024–38.
[44] iea.org [Internet]. Paris: International Energy Agency; c2022 [cited 2022 Dec 26]. Available from: https://www.iea.org/data-and-statistics/charts/development-of-co2-emission-intensity-of-electricity-generation-in-selected-countries-2000-2020.
[45] Dale PJ, Scarpulla MA. Efficiency versus effort: a better way to compare best photovoltaic research cell efficiencies? Sol Energy Mater Sol Cells 2023;251:112097.
[46] Zhao Y, Yuan S, Chang Q, Zhou Z, Kou D, Zhou W, et al. Controllable formation of ordered vacancy compound for high efficiency solution processed $Cu(In,Ga)Se_2$ solar cells. Adv Funct Mater 2021;31(10):2007928.
[47] Jeong J, Kim M, Seo J, Lu H, Ahlawat P, Mishra A, et al. Pseudo-halide anion engineering for α-$FAPbI_3$ perovskite solar cells. Nature 2021;592(7854):381–5.
[48] Apostolopoulos V, Mamounakis I, Seitaridis A, Tagkoulis N, Kourkoumpas DS, Iliadis P, et al. An integrated life cycle assessment and life cycle costing approach towards sustainable building renovation via a dynamic online tool. Appl Energy 2023;334:120710.